INTERNATIONAL JOURNAL FOR NUMERICAL METHODS IN FLUIDS
Int. J. Numer. Meth. Fluids 2008; **56**:1417–1423
Published online 24 July 2007 in Wiley InterScience (www.interscience.wiley.com). DOI: 10.1002/fld.1564

A second-order cell-centered Lagrangian scheme for two-dimensional compressible flow problems

Pierre-Henri Maire*,† and Jérôme Breil

Centre Lasers Intenses et Applications, UMR 5107 CNRS, Université Bordeaux I, CEA, 351 cours de la Libération, 33405 Talence, France

SUMMARY

This paper is devoted to the simulation of two-dimensional compressible fluid flows. We present a new second-order cell-centered scheme that solves the gas dynamics equations written in the Lagrangian formalism. The scheme is developed on general unstructured meshes consisting of arbitrary polygons. The robustness and accuracy of this new scheme are demonstrated through several test cases. Copyright © 2007 John Wiley & Sons, Ltd.

Received 23 March 2007; Revised 25 May 2007; Accepted 31 May 2007

KEY WORDS: gas dynamics equations; cell-centered Lagrangian scheme

1. INTRODUCTION

Our aim is to propose a new Lagrangian cell-centered scheme for the two-dimensional gas dynamics equations. The classical Lagrangian approach uses a staggered finite difference scheme in which velocities are vertex-centered and density, pressure and internal energy are cell-centered, see [1].

An alternative to the staggered discretization is to use a conservative cell-centered discretization in which all primary variables, including velocities, are cell-centered. The main advantage of using cell-centered velocities is the consistency among control volumes for the advection of mass, momentum and energy, in the perspective of an arbitrary Lagrangian–Eulerian extension of the Lagrangian scheme. Classical staggered discretizations do not have this consistency. However, consistent extensions have been developed for these discretizations, [2, 3].

The main difficulty with the cell-centered approach lies in the fact that the vertex velocity needed to move the mesh cannot be directly computed. In [4], the node velocity is calculated *via* a special least-squares procedure. It turns out that it leads to an artificial grid motion, which

*Correspondence to: Pierre-Henri Maire, Centre Lasers Intenses et Applications, UMR 5107 CNRS, Université Bordeaux I, CEA, 351 cours de la Libération, 33405 Talence, France.
†E-mail: maire@celia.u-bordeaux1.fr

requires a very expensive treatment [5]. Moreover, with this approach the fluxes calculation is not consistent with the node motion. Recently, a new cell-centered formulation has been proposed [6]. It is a conservative and entropy-consistent two-dimensional scheme based on a nodal solver in which the vertex velocity is computed in a coherent manner with the face fluxes. However, it appears that in the case of one-dimensional flows, this scheme leads to a nodal velocity which depends on the cell aspect ratio.

This drawback has motivated us to develop a new cell-centered scheme that solves this aspect ratio problem [7]. Our scheme computes consistently the nodal velocity and the numerical fluxes through cell interfaces. Its main feature is the introduction of four pressures on each edge, two for each node on each side of the edge. This is the main difference from [6]. Momentum and total energy conservation are ensured and the scheme satisfies a local entropy inequality. The paper is organized as follows. First, we recall the gas dynamics equations written in an integral Lagrangian form. After that, we give the spatial approximation and the nodal solver. Then, we describe briefly the second-order extension. Last, we show the accuracy and robustness of our scheme with numerical results.

2. GAS DYNAMICS EQUATIONS IN LAGRANGIAN FORM

The Lagrangian formalism consists in computing the rates of change of volume, mass, momentum and energy, assuming that the computational volumes are following the material motion. Let $\Omega(t)$ denote a control volume moving with the fluid velocity $\mathbf{V}=(u, v)^{\mathrm{t}}$, its mass constant and the Lagrangian conservation equations for volume, momentum and total energy in control volume form are

$$\frac{\mathrm{d}}{\mathrm{d}t}\int_{\Omega(t)} \mathrm{d}\Omega - \int_{\partial\Omega(t)} \mathbf{V}\cdot\mathbf{N}\,\mathrm{d}l = 0$$

$$\frac{\mathrm{d}}{\mathrm{d}t}\int_{\Omega(t)} \rho\mathbf{V}\,\mathrm{d}\Omega + \int_{\partial\Omega(t)} P\mathbf{N}\,\mathrm{d}l = \mathbf{0}$$

$$\frac{\mathrm{d}}{\mathrm{d}t}\int_{\Omega(t)} \rho E\,\mathrm{d}\Omega + \int_{\partial\Omega(t)} P\mathbf{V}\cdot\mathbf{N}\,\mathrm{d}l = 0$$

where $\partial\Omega(t)$ is the boundary of $\Omega(t)$, $\mathbf{N}$ is the unit outward normal to $\partial\Omega(t)$ and $\mathrm{d}l$ is the length element on $\partial\Omega(t)$. In these equations, ρ is the mass density, $E=\varepsilon+\frac{1}{2}\mathbf{V}\cdot\mathbf{V}$ is the specific total energy and ε is the specific internal energy. The pressure P is given as function of density ρ and internal energy ε by the equation of state. These equations are well known and have been used in this form in many papers, see, for example, [4].

3. SPATIAL APPROXIMATION

3.1. Notations and assumptions

Throughout this paper, we will use the same notations as those introduced in [2]. Let $\{c\}$ be a collection of non-overlapping polygons whose reunion covers the domain filled by the fluid. Each cell is labelled with a unique index c. We denote by $\{n\}$ the set of all the vertices of the cells. Each

DOI: 10.1002/fld

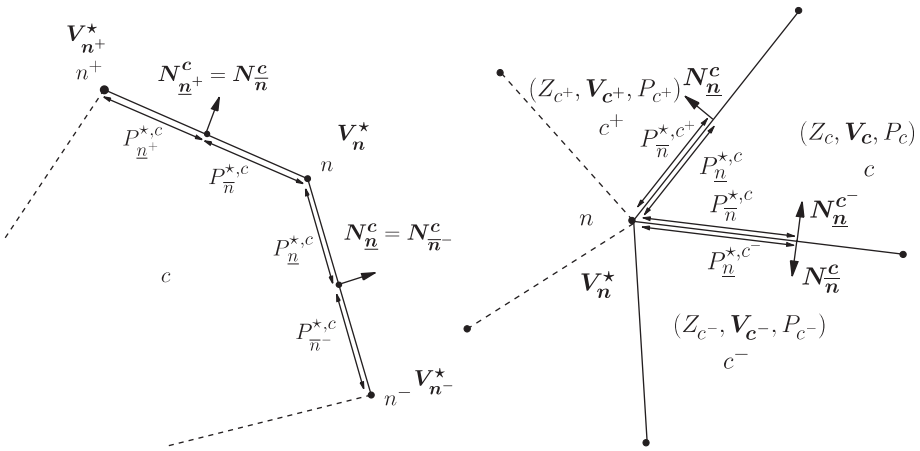

Figure 1. Notations in a cell (left) and around a node (right).

vertex is labelled with a unique index n. If we consider a given cell c, we introduce the set of all the vertices of the cell c and denote it by $\mathscr{N}(c)$. For a given node n, we also define the set of all the cells that share this vertex and denote it by $\mathscr{C}(n)$. The sets $\mathscr{N}(c)$ and $\mathscr{C}(n)$ are counterclockwise ordered. For a node $n \in \mathscr{N}(c)$, n^- and n^+ are the previous/next nodes with respect to n in the list of vertices of cell c, see Figure 1 (left). We denote by $L^c_{\underline{n}}$ and $L^c_{\overline{n}}$ the half length of the edges $[n^-, n]$ and $[n, n^+]$. We use the same notations to define the unit outward normals $\mathbf{N}^c_{\underline{n}}$ and $\mathbf{N}^c_{\overline{n}}$, see Figure 1 (left).

All fluid variables are assumed to be constant in cell c and we denote them by using subscript c. Therefore, we obtain a spatial approximation which is first-order accurate.

3.2. *Vertex fluxes*

A set of evolution equations is written for the discrete unknowns $(\tau_c, \mathbf{V}_c, E_c)$ using the Lagrangian conservation equations in control volume form applied to cell c, see [7]

$$m_c \frac{\mathrm{d}}{\mathrm{d}t}\tau_c - \sum_{n\in\mathscr{N}(c)} \left(L^c_{\underline{n}}\mathbf{N}^c_{\underline{n}} + L^c_{\overline{n}}\mathbf{N}^c_{\overline{n}}\right)\cdot \mathbf{V}^\star_n = 0 \tag{1}$$

$$m_c \frac{\mathrm{d}}{\mathrm{d}t}\mathbf{V}_c + \sum_{n\in\mathscr{N}(c)} \left(L^c_{\underline{n}}P^{\star,c}_{\underline{n}}\mathbf{N}^c_{\underline{n}} + L^c_{\overline{n}}P^{\star,c}_{\overline{n}}\mathbf{N}^c_{\overline{n}}\right) = \mathbf{0} \tag{2}$$

$$m_c \frac{\mathrm{d}}{\mathrm{d}t}E_c + \sum_{n\in\mathscr{N}(c)} \left(L^c_{\underline{n}}P^{\star,c}_{\underline{n}}\mathbf{N}^c_{\underline{n}} + L^c_{\overline{n}}P^{\star,c}_{\overline{n}}\mathbf{N}^c_{\overline{n}}\right)\cdot \mathbf{V}^\star_n = 0 \tag{3}$$

In these equations, τ_c is the specific volume and m_c is the mass in the cell c that is constant during time. $\mathbf{V}^\star_n$ denotes the nodal velocity. The main feature of our discretization is the introduction of the two pressure fluxes $P^{\star,c}_{\underline{n}}$ and $P^{\star,c}_{\overline{n}}$ at the node n, see Figure 1. $P^{\star,c}_{\underline{n}}$ (resp. $P^{\star,c}_{\overline{n}}$) represents the pressure acting between the midpoint of edge $[n^-, n]$ (resp. $[n, n^+]$) and the node n, seen from cell c. The Cartesian coordinates of node n are $\mathbf{X}_n = (X_n, Y_n)^\mathrm{t}$. The motion of the nodes is given

DOI: 10.1002/fld

by the trajectories equation $(\mathrm{d}/\mathrm{d}t)\mathbf{X}_n = \mathbf{V}_n^\star,\ \mathbf{X}_n(0) = \mathbf{x}_n$. We note that (1) is consistent with the nodes motion.

3.3. Solver at vertices

This subsection describes the way in which the vertex velocity and the pressure fluxes are determined in our scheme. Let us consider a particular node n and a cell $c \in \mathscr{C}(n)$. c^- and c^+ are the previous/next cells with respect to c in the list of cells c, see Figure 1. The fluid in cell c is characterized by $(Z_c, P_c, \mathbf{V}_c)$, where Z_c denotes the acoustic impedance defined as the product of sound velocity and density of the fluid. Let $\mathscr{V}^\star_{c^-,c}$ denote the normal velocity at the edge $[c^-, c]$ shared by cells c^- and c. This normal velocity is obtained with the approximate acoustic Riemann solver

$$\mathscr{V}^\star_{c^-,c} = \left(\frac{Z_c \mathbf{V}_c + Z_{c^-} \mathbf{V}_{c^-}}{Z_c + Z_{c^-}} \right) \cdot \mathbf{N}_{c^-,c} - \frac{P_c - P_{c^-}}{Z_c + Z_{c^-}} \tag{4}$$

where $\mathbf{N}_{c^-,c} = \mathbf{N}_{\underline{n}}^{c^-} = -\mathbf{N}_{\overline{n}}^{c}$ is the unit normal at the edge $[c^-, c]$. The nodal velocity is computed from the following least-squares procedure. $\mathbf{V}_n^\star = (u_n^\star, v_n^\star)^{\mathrm{t}}$ is the vector that minimizes the functional

$$I(u_n^\star, v_n^\star) = \sum_{c^-,c} \omega_{c^-,c} (\mathbf{V}_n^\star \cdot \mathbf{N}_{c^-,c} - \mathscr{V}^\star_{c^-,c})^2 \tag{5}$$

In this equation, the sum is made over all the edges impinging on node n and $\omega_{c^-,c}$ denotes the weight corresponding to the edge $[c^-, c]$. This weight will be evaluated in the sequel. The least-squares problem is posed by the equation $\nabla I = \mathbf{0}$ where $\nabla I = (\partial I/\partial u_n^\star, \partial I/\partial v_n^\star)^{\mathrm{t}}$. This yields the vectorial equation

$$\sum_{c^-,c} \omega_{c^-,c} (\mathbf{V}_n^\star \cdot \mathbf{N}_{c^-,c} - \mathscr{V}^\star_{c^-,c}) \mathbf{N}_{c^-,c} = \mathbf{0} \tag{6}$$

For given non-negative weights, this equation admits always a well-defined solution. Then, knowing the nodal velocity, we define the pressure fluxes in the following way:

$$P_{c^-} - P_{\underline{n}}^{\star,c^-} = Z_{c^-} (\mathbf{V}_n^\star - \mathbf{V}_{c^-}) \cdot \mathbf{N}_{c^-,c} \tag{7}$$

$$P_c - P_{\overline{n}}^{\star,c} = -Z_c (\mathbf{V}_n^\star - \mathbf{V}_c) \cdot \mathbf{N}_{c^-,c} \tag{8}$$

If we subtract (8) from (7), after straightforward calculations, one gets $P_{\overline{n}}^{\star,c} - P_{\underline{n}}^{\star,c^-} = (Z_c + Z_{c^-})(\mathbf{V}_n^\star \cdot \mathbf{N}_{c^-,c} - \mathscr{V}^\star_{c^-,c})$. Since, in general, we have $\mathbf{V}_n^\star \cdot \mathbf{N}_{c^-,c} \neq \mathscr{V}^\star_{c^-,c}$ then $P_{\overline{n}}^{\star,c} \neq P_{\underline{n}}^{\star,c^-}$ and we lose momentum conservation contrary to classical finite volume approaches. Nonetheless, we can show that momentum conservation can be recovered provided the weight $\omega_{c^-,c}$ is given by

$$\omega_{c^-,c} = L_{c^-,c} (Z_c + Z_{c^-}) \tag{9}$$

We recall that the weights used for the least-squares problem in [4] are the inverse of the side lengths and consequently are very different from those we have obtained here. With this choice and the definition of the pressure fluxes, (6) becomes

$$\sum_{c \in \mathscr{C}(n)} (L_{\underline{n}}^c P_{\underline{n}}^{\star,c} \mathbf{N}_{\underline{n}}^c + L_{\overline{n}}^c P_{\overline{n}}^{\star,c} \mathbf{N}_{\overline{n}}^c) = \mathbf{0} \tag{10}$$

DOI: 10.1002/fld

Finally, we obtain momentum and also total energy conservation. Knowing the weights $\omega_{c^-,c}$, the nodal velocity is obtained by solving (6). One can verify that with these fluxes the entropy production rate in the cell c is always positive. Thus, our scheme satisfies a local entropy inequality, see [7] for the detailed proof.

Our scheme computes in a coherent way the vertex motion as well as the face fluxes. It is shown in [7] that the nodal solver recovers the one-dimensional acoustic solver in the case of one-dimensional planar and cylindrical flows, contrary to the scheme derived in [6]. The boundary conditions are easily derived using the same methodology, see [7].

4. SECOND-ORDER EXTENSION

The spatial second-order extension is obtained by a piecewise linear monotonic reconstruction of the pressure and velocity, given by their mean values over mesh cells. This reconstruction utilizes a least-squares procedure, see [8]. We define slope limiters in such a way that the values of the linear function at the cell vertices are within the bounds defined by the maximum and the minimum of the mean values over the set consisting of cell c and its nearest neighbors, see [8]. Finally, instead of using the mean values of the pressure and the velocity in our nodal solver, we use their nodal extrapolated values deduced from the linear reconstruction. The time discretization is explicit and is based on a classical two-step Runge–Kutta procedure.

5. NUMERICAL RESULTS

5.1. *Noh problem on a Cartesian grid*

A perfect gas with $\gamma = \frac{5}{3}$ is given an initial unit inward radial velocity. The initial thermodynamic state is given by $(\rho, P) = (1, 0)$. The initial domain is a square of unit length. We use a Cartesian grid defined by a mesh of 50×50 cells. In Figure 2 (left), we can observe the high quality of the

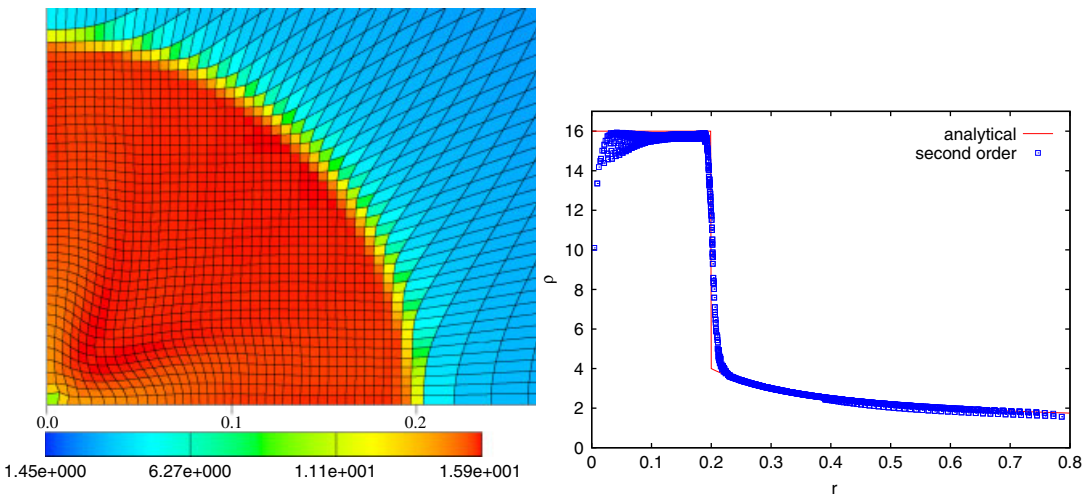

Figure 2. Noh problem, density map (left) and density in all cells (right) at $t = 0.6$.

DOI: 10.1002/fld

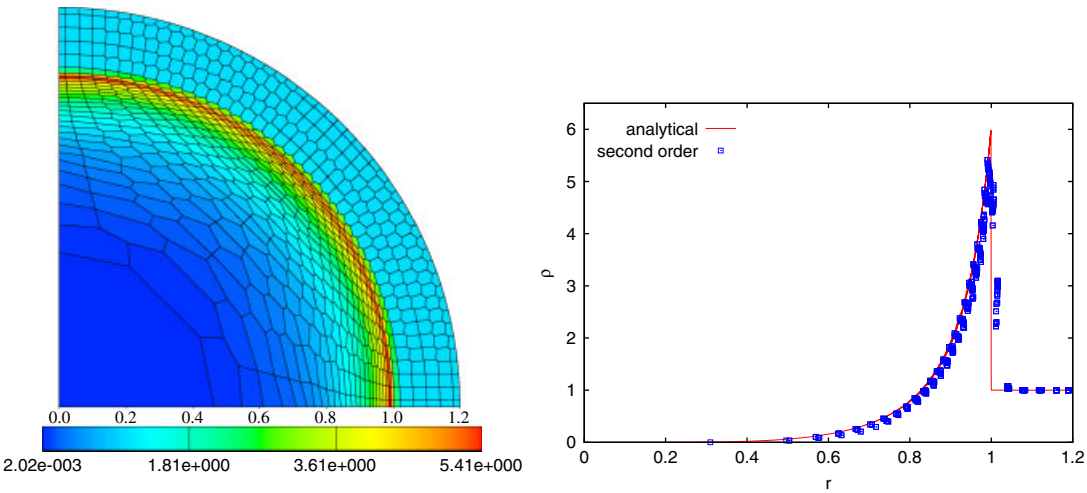

Figure 3. Sedov problem (polygonal grid), density map (left) and density in all cells (right) at $t = 1$.

mesh after shock reflection. For the density, we obtain a very good agreement with the analytical solution, see Figure 2 (right).

5.2. *Sedov problem on a polygonal grid*

This test case describes the evolution of a blast wave in a point symmetric explosion. We present numerical results obtained with the data and the polygonal grid defined in [2]. In Figure 3, we observe a good agreement with the analytical solution for the density. The numerical solution preserves very well the cylindrical symmetry. This result shows the ability of our scheme to handle unstructured meshes.

6. CONCLUSIONS

This new second-order cell-centered Lagrangian method looks promising not only as a stand-alone entity but also as a foundation for arbitrary Lagrangian–Eulerian method. The uniform cell centering of the solution variables provides a consistent basis for employing a wide range of well-proven remapping and adaptation schemes. Our future works will be on the multimaterial ALE extension and the three-dimensional extension of our Lagrangian scheme.

REFERENCES

1. Caramana EJ, Burton DE, Shashkov MJ, Whalen PP. The construction of compatible hydrodynamics algorithms utilizing conservation of total energy. *Journal of Computational Physics* 1998; **146**:227–262.
2. Loubère R, Shashkov MJ. A subcell remapping method on staggered polygonal grids for arbitrary-Lagrangian–Eulerian methods. *Journal of Computational Physics* 2005; **209**:105–138.
3. Benson DJ. Momentum advection on a staggered mesh. *Journal of Computational Physics* 1992; **100**:143–162.

DOI: 10.1002/fld

4. Adessio FL, Carroll DE, Dukowicz JK, Harlow FH, Johnson JN, Kashiwa BA, Maltrud ME, Ruppel HM. CAVEAT: a computer code for fluid dynamics problems with large distortion and internal slip. *Report LA-10613-MS*, Los Alamos National Laboratory, 1986.
5. Dukowicz JK, Meltz B. Vorticity errors in multidimensional Lagrangian codes. *Journal of Computational Physics* 1992; **99**:115–134.
6. Després B, Mazeran C. Lagrangian gas dynamics in two dimensions and Lagrangian systems. *Archive for Rational Mechanics and Analysis* 2005; **178**:327–372.
7. Abgrall R, Breil J, Maire P-H, Ovadia J. A cell-centered Lagrangian scheme for two-dimensional compressible flow problems. *SIAM Journal on Scientific Computing* 2007, to appear, http://hal.inria.fr/inria-00113542.
8. Barth T. *Numerical Methods for Conservation Laws on Structured and Unstructured Meshes*. VKI Lecture Series, 2003. Available at http://people.nas.nasa.gov/∼barth/vki_ls2003/barth_2003_vki_lecture_series.pdf.

DOI: 10.1002/fld